

Experimental Comparison of Online Parameter Identification Schemes for a Nanopositioning Stage with Variable Mass

Arnfinn Aas Eielsen, Tomáš Polóni, Tor Arne Johansen, and Jan Tommy Gravdahl

Abstract—An experimental comparison of two common parameter identification schemes is presented. The recursive least squares method and the extended Kalman filter are applied to identify three parameters of a second-order linear mass-spring-damper model, using data obtained from a nanopositioning stage with a highly resonant dynamic response.

I. INTRODUCTION

Applying damping control to highly resonant flexible structures, one can often find optimal controller parameters that will maximize the introduced damping [1], [2], [3]. Finding the optimal controller parameters requires knowledge of the dynamics of the flexible structure at hand. An accurate description of the dynamics can often be obtained from e.g. frequency response data, and the optimal controller parameters can for instance be found using some optimization scheme incorporating these data. In some applications system parameters can be expected to change during operation, and controller parameters should be adjusted accordingly to maintain optimal damping.

Nanopositioning stages often exhibit highly resonant dynamics. Such devices are typically used for high precision positioning, found in systems for scanning probe microscopy, optical alignment, and data storage [4].

In order to obtain higher precision, damping control (feedback) can be employed as part of the control scheme to good effect [5], or feed-forward compensation using the inverse kinematics can be used [6]. Since the application of nanopositioning stages typically involve moving payloads of various masses, the resonance frequencies of the mechanical structure will change every time a new payload is attached. In addition, such devices will most frequently use piezoelectric actuators, which will experience variation in gain due to changes in actuator temperature, as well as introduce disturbances due to hysteresis and creep [4].

It is apparent that control schemes for such devices can benefit from some form of online adaptation in order to

This work was supported by the Norwegian Research Council and the Norwegian University of Science and Technology. The second author is supported by the Slovak Research and Development Agency under projects APVV-0090-10 and LPP-0118-09.

Arnfinn Aas Eielsen eielsen@itk.ntnu.no, Tor Arne Johansen tor.arne.johansen@itk.ntnu.no, and Jan Tommy Gravdahl jan.tommy.gravdahl@itk.ntnu.no are with the Department of Engineering Cybernetics at the Norwegian University of Science and Technology, Trondheim, Norway

Tomáš Polóni tomas.poloni@stuba.sk is with the Institute of Automation, Measurement and Applied Informatics at the Slovak University of Technology, Bratislava, Slovakia

maintain optimal performance during operation.

As a step in this direction, two common schemes for parameter identification have been compared experimentally in order to assess their ability to learn the model parameters for a simple second-order linear model for the vibration dynamics (a mass-spring-damper system) in open-loop. The schemes are the recursive least squares method (RLS) and two different versions of the extended Kalman filter (EKF), continuous EKF and hybrid EKF.

In Section II the system is described, followed by brief introductions to the RLS in Section III, and the continuous EKF and hybrid EKF in Section IV. The experiments are described in Section V, and the results from the experiments are presented in Section VI, followed by a discussion Section VII and conclusions in Section VIII.

II. SYSTEM DESCRIPTION

A. Mechanical Model

The dynamics of flexible structures are often adequately described by lumped parameter truncated linear models [1]. The most pronounced vibrations modes will typically be included in such a model, while higher order modes with small response magnitudes are neglected. A general model form to describe the dynamics for n point masses in the presence of external and linear elastic, inertia and damping



Fig. 1. Nanopositioning stage.

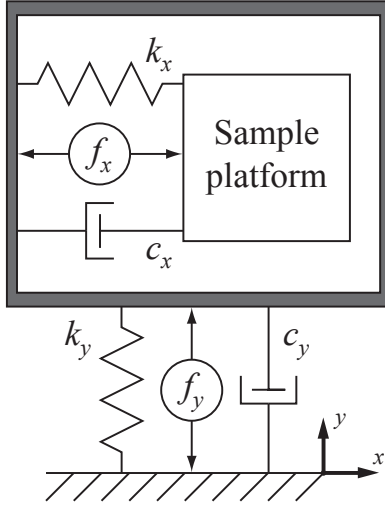


Fig. 2. Serial-kinematic configuration of the nanopositioning stage.

forces, in a non-gyroscopic, flexible structure is

$$M\ddot{x} + C\dot{x} + Kx = f$$

where $x \in \mathbb{R}^n$ is the vector of displacements, $f \in \mathbb{R}^m$ is the vector of external point forces, M , C , and K are, respectively, the mass, damping and stiffness matrices. The mass, damping, and stiffness matrices are symmetric and semi-positive definite.

The nanopositioning stage used in this work is shown in Fig. 1. It has a serial-kinematic configuration. A simplified free body diagram for the mechanism is displayed in Fig. 2.

Motion along the y -axis is considered. The dynamic model for the displacement x_y is

$$m_y\ddot{x}_y + c_y\dot{x}_y + k_yx_y = f_y,$$

where m_y (kg) will be the compound mass of the sample platform and the actuation mechanism for the x -axis, as well as mass due to any payload attached to the sample platform, c_y (Ns/m) is the damping coefficient, k_y (N/m) is the spring constant, and f_y (N) is the applied external force.

The piezoelectric actuator can be considered a force transducer, generating a force proportional to the applied voltage, thus the external force applied in the y -direction is given by

$$f_y = \beta u$$

where β (N/V) is the effective gain of the piezoelectric actuator from voltage to force, and u (V) is the applied voltage.

Dropping the y -subscripts, and denoting $x_1 = x_y$, the state-space formulation for the system is given as

$$\begin{aligned} \dot{x}_1 &= x_2 \\ \dot{x}_2 &= -a_0x_1 - a_1x_2 + b_0u, \end{aligned} \quad (1)$$

where $a_0 = \frac{k}{m}$ ($1/s^2$), $a_1 = \frac{c}{m}$ ($1/s$), and $b_0 = \frac{\beta}{m}$ (m/s^2V).

The frequency response for this axis was recorded, using bandwidth-limited white noise excitation, with and without a

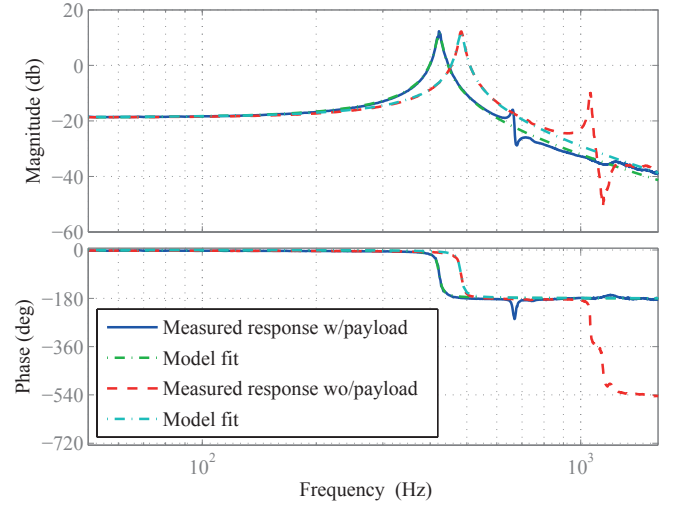


Fig. 3. Measured frequency response for one axis of the nanopositioning stage, and the corresponding response using the model (1) and parameter values from Table I, with and without payload attached to the sample platform.

payload of approx. 24.75 g attached to the sample platform. The two responses are displayed in Fig. 3. The model (1) was fitted to the frequency response data using the MATLAB System Identification Toolbox, and the resulting parameter values are presented in Tab. I, and the response of the model (1) using these parameters are also displayed in Fig. 3.

As can be seen, the actual response of the first vibration mode is well approximated by the model. There are higher order modes in the system, and the second vibration mode is clearly visible in Fig. 3. The higher order modes have negligible magnitude responses in comparison to the first, thus a second-order model should be sufficient to describe the dominant dynamics of the system.

We note that the parameters in Tab. I translates to a natural frequency of $f_0 = \sqrt{a_0}/2\pi = 423$ Hz and a damping ratio of $\zeta = a_1/2\sqrt{a_0} = 0.0146$ for the case with the payload attached, and for the case without the payload, we have a natural frequency of $f_0 = 483$ Hz and a damping ratio of $\zeta = 0.0143$. The dc-gain for the case with payload is $\frac{b_0}{a_0} = 0.114$ $\mu\text{m/V}$, and for the case without payload it is $\frac{b_0}{a_0} = 0.116$ $\mu\text{m/V}$.

TABLE I
IDENTIFIED PARAMETERS FOR THE MODEL (1), USING FREQUENCY RESPONSE DATA.

With payload on sample platform		
Parameter	Value	Unit
b_0	$0.808 \cdot 10^6$	$\mu\text{m/s}^2\text{V}$
a_0	$7.06 \cdot 10^6$	$1/s^2$
a_1	77.6	$1/s$
Without payload on sample platform		
Parameter	Value	Unit
b_0	$1.07 \cdot 10^6$	$\mu\text{m/s}^2\text{V}$
a_0	$9.21 \cdot 10^6$	$1/s^2$
a_1	86.8	$1/s$

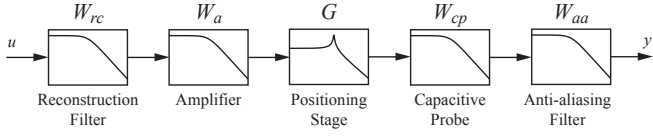


Fig. 4. Signal chain for the overall system.

B. Overall System

The complete system used consisted of the nanopositioning stage, as well as a reconstruction filter, an anti-aliasing filter, an amplifier and a displacement sensor (a capacitive probe). The signal chain is shown schematically in Fig. 4.

The sampling frequency used was 10 kHz. The reconstruction and anti-aliasing filters were configured as second-order low-pass Butterworth filters with conservative cut-off frequencies at 1 kHz. The amplifier, with the given capacitive load of the piezoelectric actuator, provided a bandwidth of approximately 10 kHz, and the displacement sensor was configured with a bandwidth of 100 kHz.

As the reconstruction and anti-aliasing filters noticeably impact the observed dynamics, these were taken into account when generating the input signal for the identification schemes, as shown in Fig. 5. This ensured that the input signal u' would match the output signal y' in phase and magnitude, in a sense removing the effect of these filters. The effects of the amplifier and the displacement sensor were neglected, as it would be impossible to implement replicas of these filters digitally with the chosen sampling frequency.

To improve the results obtained from the parameter identification schemes, a pre-filter, W_p , was used. This was chosen with consideration to the sensitivity functions for the parameters of the model. For a transfer function $G(s)$, the Bode sensitivity function with respect to some parameter θ , is defined as

$$S_{\theta}^{G(s)} \triangleq \frac{\partial G(s)/G(s)}{\partial \theta/\theta} = \frac{\theta_0}{G(s)_0} \frac{\partial G(s)}{\partial \theta} \Big|_{\text{NOP}},$$

using a nominal operating point (NOP) for all the parameters in the transfer function [7].

The sensitivity functions for the parameters b_0 , a_0 , and a_1 in the system model (1), using the parameters with payload as the NOP, are displayed in Fig. 6. Most notably, the parameter related to damping, a_1 , has very little impact on the observed output at low and high frequencies. For parameter identification it is considered good practice to concentrate signal power in the frequency domains that contain peaks in the sensitivity functions. This is done in order to maximize the information content of the signals used [8], [9].

The pre-filter was chosen to be a band-pass filter, using a first-order high-pass filter with lower cut-off frequency of $f_{lc} = 100$ Hz, and a resonant second-order low-pass filter, with natural frequency of $f_0 = 450$ Hz, and a damping ratio of $\zeta = 0.1$, thus amplifying the frequency content close to the

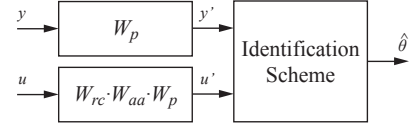


Fig. 5. Signals fed to identification schemes.

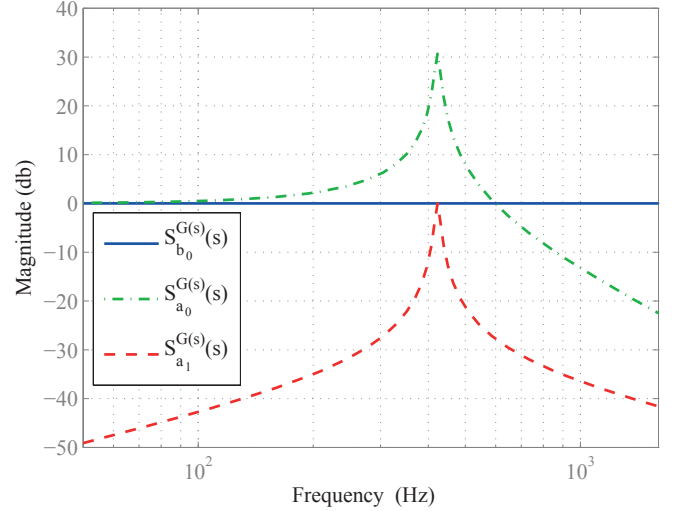


Fig. 6. Sensitivity functions for the parameters b_0 , a_0 , and a_1 , using data from Tab. I.

resonant peaks of the two configurations (with and without payload):

$$W_p(s) = \frac{s}{s + 2\pi f_{lc}} \frac{(2\pi f_0)^2}{s^2 + 2\zeta\pi f_0 s + (2\pi f_0)^2}$$

When applying the RLS method, numerical first and second derivatives of the displacement signal are needed. In order to generate proper transfer functions for filtering the displacement signal, the low-pass filter was chosen to be second order. To keep the order of the pre-filter at a minimum, the high-pass filter was chosen to be first-order.

III. RECURSIVE LEAST SQUARES METHOD

The least squares method [10] is perhaps the best known method for parameter identification. It can be used in recursive and non-recursive form.

The starting point is a model of the system, assuming the measured response y can be described as a vector of model parameters θ appearing affinely with a vector of known signals, φ , called the regressor:

$$y = \theta^T \varphi$$

The objective of the method is to find a good estimate of the vector of parameter values, $\hat{\theta}$. By computing the estimated response

$$\hat{y} = \hat{\theta}^T \varphi$$

we can form the estimate error ϵ as

$$\epsilon = \frac{y - \hat{y}}{m^2}$$

where m^2 is a normalization signal (defined below) to ensure that the estimate error will be bounded, i.e. $\epsilon \in \mathcal{L}_\infty$. The (pure) least squares estimate of the parameters is then obtained when minimizing the cost-function:

$$J(\hat{\theta}) = \frac{1}{2} \left[\int_0^t \epsilon^2 d\tau + (\hat{\theta} - \hat{\theta}_0)^T Q_0 (\hat{\theta} - \hat{\theta}_0) \right] \quad (2)$$

The matrix Q_0 is used to weigh the significance of the initial parameter estimates, $\hat{\theta}_0$, in minimizing the cost-function. The cost-function (2) does not guarantee exponential convergence of $\hat{\theta}$ to θ . By adding exponential discounting of past data, by introducing a forgetting factor γ , exponential convergence can be achieved. The cost-function will then be:

$$J(\hat{\theta}) = \frac{1}{2} \left[\int_0^t e^{-\gamma(t-\tau)} \epsilon^2 d\tau + e^{-\gamma t} (\hat{\theta} - \hat{\theta}_0)^T Q_0 (\hat{\theta} - \hat{\theta}_0) \right]$$

The above expressions can be used to derive both the recursive and the non-recursive form of the least squares method. Here we apply the recursive form, amenable to online implementation. The parameter update law is then given by:

$$\dot{\hat{\theta}} = P\epsilon\varphi, \quad \theta(0) = \theta_0$$

The matrix P is called the covariance matrix, and can be found by computing e.g.

$$\dot{P} = \begin{cases} \gamma P - \frac{P\varphi\varphi^T P}{m^2}, & \text{if } \|P\| \leq R_0 \\ 0 & \text{otherwise} \end{cases}, \quad P(0) = Q_0^{-1}.$$

The initial covariance matrix must be symmetric and positive definite, $P(0) = Q_0^{-1} = Q_0^{-T} > 0$. By using the forgetting factor γ when updating the covariance P , there is a possibility for P to grow without bound, thus $\|P\|$ is bounded by R_0 . The initial covariance matrix should therefore also satisfy $\|P(0)\| \leq R_0$.

The normalization signal m^2 can be constructed in various ways to achieve boundedness of ϵ . Here it is taken to be

$$m^2 = 1 + n_s^2, \quad n_s^2 = \varphi^T P \varphi.$$

This method is referred to as the modified least-squares with forgetting factor. It has the properties $\epsilon, \epsilon n_s, \hat{\theta}, \hat{\theta} \in \mathcal{L}_\infty$ and $\epsilon, \epsilon n_s, \hat{\theta} \in \mathcal{L}_2$. In addition, if the regressor φ is persistently exciting (PE), then $\hat{\theta}$ converges exponentially to θ . A piecewise continuous signal vector $\varphi : \mathbb{R}^+ \rightarrow \mathbb{R}^n$ is said to be PE in \mathbb{R}^n with a level of excitation α_0 if there exists constants $\alpha_1, T_0 > 0$ such that

$$\alpha_1 I \geq \frac{1}{T_0} \int_t^{t+T_0} \varphi\varphi^T d\tau \geq \alpha_0 I, \quad \forall t \geq 0.$$

For linear single-input-single-output systems, such as the one used in this work, as PE regressor vector is obtained if the input signal u is sufficiently rich. In brief, an input signal is sufficiently rich if it contains more frequency components than half the number of unknown parameters [10].

For the system (1), we have the parameter vector

$$\theta = [b_0, a_1, a_0]^T,$$

the regressor vector is

$$\varphi = [u, -x_2, -x_1]^T,$$

and the output of the model is $y = \dot{x}_2$.

IV. EXTENDED KALMAN FILTER

The extended Kalman filter [11], [12], [13] has become a popular method for recursive parameter identification. It is based on a weighted least squares criterion, but unlike the RLS method, the states of the system are estimated as well as the parameters.

A. Continuous Extended Kalman Filter

A general non-linear system is described by

$$\begin{aligned} \dot{x} &= f(x, u) + w \\ y &= h(x) + v \end{aligned} \quad (3)$$

where $x \in \mathbb{R}^n$ are the states, $y \in \mathbb{R}^m$ are the measurements, $u \in \mathbb{R}^l$ is the input, and w and v are zero-mean Gaussian white noise processes, described uniquely by the process noise covariance matrix Q , and the measurement noise covariance matrix R , respectively:

$$\begin{aligned} E[w(t)w(\tau)^T] &= Q\delta(t - \tau) \\ E[v(t)v(\tau)^T] &= R\delta(t - \tau) \end{aligned}$$

The extended Kalman filter (EKF) is obtained when the states of the system (3) are estimated by linearizing about the Kalman filter's estimated trajectory. Linearization is done by computing the Jacobians

$$\begin{aligned} F &= \left. \frac{\partial f}{\partial x} \right|_{\hat{x}}, \\ H &= \left. \frac{\partial h}{\partial x} \right|_{\hat{x}}. \end{aligned}$$

Now the state estimates \hat{x} can be computed by solving

$$\begin{aligned} \hat{x}(0) &= E[x(0)] \\ P(0) &= E[(x(0) - \hat{x}(0))(x(0) - \hat{x}(0))^T] \\ \dot{\hat{x}} &= f(\hat{x}, u) + K[y - h(\hat{x})] \\ K &= PH^T R^{-1} \\ \dot{P} &= FP + PF^T + Q - KHP, \end{aligned}$$

where P is the error covariance, and K is the Kalman gain. The above recursion is equivalent to minimizing the cost function

$$\begin{aligned} J(\hat{x}) &= \frac{1}{2} (\hat{x} - \hat{x}(0))^T P(0)^{-1} (\hat{x} - \hat{x}(0)) \\ &+ \frac{1}{2} \int_0^t (y - h(\hat{x}))^T R^{-1} (y - h(\hat{x})) + w^T Q^{-1} w d\tau \end{aligned}$$

subject to $\dot{x} = f(x, u) + w$ [11], [14]. Summarily; large measurement noise covariances will penalize the use of measurements, and large process noise covariances will penalize the use of predicted states from the system model. $P(0)^{-1}$ has the same effect as Q_0 in (2).

The extended Kalman filter can be used for parameter identification, by modeling unknown parameters as Wiener processes. Consider the linear system

$$\begin{aligned}\dot{x} &= A(\theta)x + B(\theta)u + w \\ y &= C(\theta)x + v\end{aligned}$$

with unknown parameters $\theta \in \mathcal{R}^p$. By augmenting the state vector to include the unknown parameters, $\chi^T = [x^T, \theta^T]$, we obtain the non-linear system $\dot{\chi} = f(\chi, u) + w$, $y = h(\chi) + v$, where

$$\begin{aligned}f(\chi, u) &= \begin{bmatrix} A(\theta)x + B(\theta)u \\ 0 \end{bmatrix} \\ h(\chi) &= C(\theta)x.\end{aligned}$$

The Jacobians F and H for this system are found as

$$\begin{aligned}F &= \begin{bmatrix} A(\theta) & \frac{\partial}{\partial \theta}[A(\theta)x + B(\theta)u] \\ 0 & 0 \end{bmatrix}_{\hat{x}, \hat{\theta}}, \\ H &= \begin{bmatrix} C(\theta) & \frac{\partial}{\partial \theta}[C(\theta)x] \end{bmatrix}_{\hat{x}, \hat{\theta}}.\end{aligned}$$

Applying the EKF to the model (1), we have

$$\chi = \begin{bmatrix} x \\ \theta \end{bmatrix} = [x_1 \quad x_2 \quad a_0 \quad a_1 \quad b_0]^T,$$

$$A(\theta) = \begin{bmatrix} 0 & 1 & 0 & 0 & 0 \\ -a_0 & -a_1 & 0 & 0 & 0 \\ 0 & 0 & 0 & 0 & 0 \\ 0 & 0 & 0 & 0 & 0 \\ 0 & 0 & 0 & 0 & 0 \end{bmatrix}, \quad B(\theta) = \begin{bmatrix} 0 \\ b_0 \\ 0 \\ 0 \\ 0 \end{bmatrix},$$

$$C(\theta) = [1 \quad 0 \quad 0 \quad 0 \quad 0],$$

$$F = \begin{bmatrix} 0 & 1 & 0 & 0 & 0 \\ -a_0 & -a_1 & -x_1 & -x_2 & u \\ 0 & 0 & 0 & 0 & 0 \\ 0 & 0 & 0 & 0 & 0 \\ 0 & 0 & 0 & 0 & 0 \end{bmatrix}, \quad \text{and } H = C.$$

B. Hybrid Extended Kalman Filter

A more accurate model of the system could have been obtained by using an exact discretization, but by implementing a discrete EKF using such a model, there will be the added complexity of finding the transition matrix of the system and the required Jacobians. Instead, applying a continuous-discrete, or hybrid, version of the EKF (HEKF) [11], [12] might improve the accuracy of the estimates, since the continuous part of the method can be run at a higher rate than the sampling rate. The predicted system response will therefore be closer to the response one would get if exact discretization was used, but while using the setup already found for the continuous EKF.

The system response is now described by the hybrid system

$$\begin{aligned}\dot{x} &= f(x, u_k) + w \\ y_k &= h(x_k) + v_k\end{aligned}$$

where y_k is sampled sequence of measurements, u_k is the input sequence, and v_k is a Gaussian white noise sequence, and the noise properties are given by

$$\begin{aligned}E[w(t)w(\tau)^T] &= Q\delta(t - \tau) \\ E[v_k v_i^T] &= R_d \delta_{ki}\end{aligned}$$

where $R_d \approx R/T$, and T is the sampling period. Using the initial values

$$\hat{x}_0 = E[x(0)] \quad \text{and} \quad P_0 = E[(x(0) - \hat{x}_0)(x(0) - \hat{x}_0)^T],$$

the state estimates \hat{x}_k for $k = 1, 2, \dots$ are computed by the hybrid EKF in two parts.

(1) The a priori state estimates and error covariance, from time-step $k - 1$ to k^- (i.e. for the sampling period T), are found solving

$$\begin{aligned}\dot{x} &= f(x, u_{k-1}) \\ \dot{P} &= FP + PF^T + Q\end{aligned}$$

where the initial values are given by $\hat{x}(0) = \hat{x}_{k-1}$ and $P(0) = P_{k-1}$.

(2) Given the a priori estimates $\hat{x}_k^- = \hat{x}(T)$ and error covariance $P_k^- = P(T)$, the a posteriori state estimates \hat{x}_k and error covariance P_k are found computing:

$$\begin{aligned}K_k &= P_k^- H^T (H P_k^- H^T + R_d)^{-1} \\ \hat{x}_k &= \hat{x}_k^- + K_k (y_k - h(\hat{x}_k^-)) \\ P_k &= (I - K_k H) P_k^- (I - K_k H) + K_k R_d K_k^T\end{aligned}$$

C. Convergence Properties

In contrast to the RLS method, which has a firm theoretical foundation with regards to parameter convergence in the presence of a sufficiently rich input signal [10], [8], there does not exist any general proof of convergence for the EKF. The EKF can provide good performance, though, but the quality of the estimates and convergence are susceptible to the choice of initial values and covariance tuning, as well as the input signal [15], [16], [17], [12]. Theoretically, the RLS method should converge to the correct parameter values when using a sufficiently rich input signal (which results in a PE regressor vector). In practice, this might not happen.

V. EXPERIMENTS

A. Instrumentation

The experiment setup consisted of the long-range serial-kinematic nanopositioning stage from easyLab, already described in Section II, as well as a Piezodrive PDL200 linear voltage amplifier (20 V/V), a ADE 6810 capacitive gauge and ADE 6501 capacitive probe from ADE Technologies to measure displacement (5 $\mu\text{m/V}$), and two SIM 965 programmable filters from Stanford Research Systems, used as reconstruction and anti-aliasing filters. The actuation signal and measured response was generated and recorded using a dSPACE DS1103 hardware-in-the-loop board, at a sampling frequency of 10 kHz.

The capacitance of the piezoelectric actuator was measured to be $C_p \approx 700$ nF, thus the amplifier would, according to the specifications, provide a first-order low-pass filter dynamic response with a cut-off frequency of 10 kHz. The specifications for the capacitive gauge and probe state that the response should be like a first-order low-pass filter with a cut-off frequency of 100 kHz. The programmable filters were both configured as second-order Butterworth filters with cut-off frequencies at 1 kHz.

B. Performed Experiments

Two experiments were performed. One using a pseudo random binary signal (PRBS) [8] as the input to the system, and one using a more typical signal for this particular kind of device, i.e. a smoothed triangle wave [18]. The PRBS was generated to provide frequency content in the band from 0 to 1 kHz. The triangle wave signal had a fundamental frequency of 10 Hz. Both signals had an amplitude of 1 V.

The PRBS yielded large excitations, and thus provided an ideal response with regards to parameter identification. The triangle wave signal, on the other hand, yielded very little excitation of the dynamics of the system, and therefore provided a much more challenging task for the parameter identification schemes.

Both experiments were performed by first attaching the payload, a small block of steel weighing 24.75 g, to a magnet fixed to the sample platform. Measurements of the displacement were then recorded for approx. 100 seconds with the payload attached, before the payload was removed (while the system was running), and approx. 100 seconds more was recorded with the payload detached.

C. Implementation and Tuning

For all methods the fourth-order Runge-Kutta scheme [19] was used for numerical integration of continuous-time differential equations. All methods were initialized with the initial parameter estimates¹:

$$\theta_0 = [b_0, a_1, a_0]_0^T = [5 \cdot 10^5, 7 \cdot 10^1, 6 \cdot 10^6]^T$$

For the EKFs, the initial state estimates were set to zero.

1) *RLS*: The applied RLS method provides two tuning parameters, the forgetting factor γ , and the initial covariance matrix $P(0)$. The initial covariance matrix will only affect the initial transient of the parameter estimates, thus, convergence speed is mostly determined by γ . We found that the maximal forgetting factor that did not make the norm of the covariance matrix P to grow excessively large, was about $\gamma = 0.25$. The initial covariance matrix was set to:

$$P(0) = \text{diag}([1 \cdot 10^6, 1 \cdot 10^1, 1 \cdot 10^7])$$

¹Note that in our implementation $\theta = [b_0, a_1, a_0]^T$ for RLS, and $\theta = [a_0, a_1, b_0]^T$ for EKF.

2) *Continuous EKF and Hybrid EKF*: The EKFs required tuning of the covariance matrices, R , Q , and $P(0)$. The measurement noise variance was found to be $\sigma_y^2 \approx 1.5 \cdot 10^{-6}$, thus the measurement covariance matrix was set to $R = \sigma_y^2 I$ for the continuous EKF, and $R_d = R/T$ for the hybrid EKF. The process noise covariance matrix was tuned using the more challenging dataset obtained using the triangle wave excitation, and good results were obtained when using:

$$Q_1 = \text{diag}([1 \cdot 10^{-12}, 1 \cdot 10^{-6}, 1.5 \cdot 10^{11}, 2.5 \cdot 10^1, 5.0 \cdot 10^{10}])$$

When using PRBS excitation, the variances in the parameter estimates were very large when using the above tuning, but this was improved by reducing the covariances for the parameters, i.e.:

$$Q_2 = \text{diag}([1 \cdot 10^{-12}, 1 \cdot 10^{-6}, 1.5 \cdot 10^9, 2.5 \cdot 10^{-1}, 5.0 \cdot 10^8])$$

The initial error covariance matrix was set to:

$$P(0) = 10 \cdot Q_i$$

In the hybrid EKF, the continuous part was run at a faster rate than the sampling frequency. We found that a step length, for both datasets, of $T/4$, to produce good results (yielding a rate of 40 kHz).

VI. EXPERIMENTAL RESULTS

A. Parameter Estimates

The parameter estimates when using triangle wave excitation signal are presented in Fig. 7, and the parameter estimates when using PRBS excitation are shown in Fig. 8.

To obtain some form of validation of the parameter estimates, we used the following procedure: The mean value of each parameter estimate time-series was computed for $t_1 \in (75, 100)$ s and $t_2 \in (175, 200)$ s. Using these values, the response of the model (1) was computed for t_1 and t_2 , using the input signal and mass configuration the parameter values were found for. The simulated responses was then compared to the measured responses. Tab. II summarizes the resulting root-mean-square-errors (RMSE). The RMSE when using the values in Tab. I are also shown.

TABLE II
RMSE OF SIMULATED VS. MEASURED RESPONSES IN mm.
MEASUREMENT NOISE IS APPROX. 1.25 nm RMS.

	EKF	RLS	HEKF	Tab. I
With payload on sample platform				
PRBS	20.5	70.8	72.4	96.9
Triangle Wave	1.66	1.67	1.65	1.92
Without payload on sample platform				
PRBS	29.9	81.7	70.8	31.7
Triangle Wave	1.68	1.72	1.68	2.44

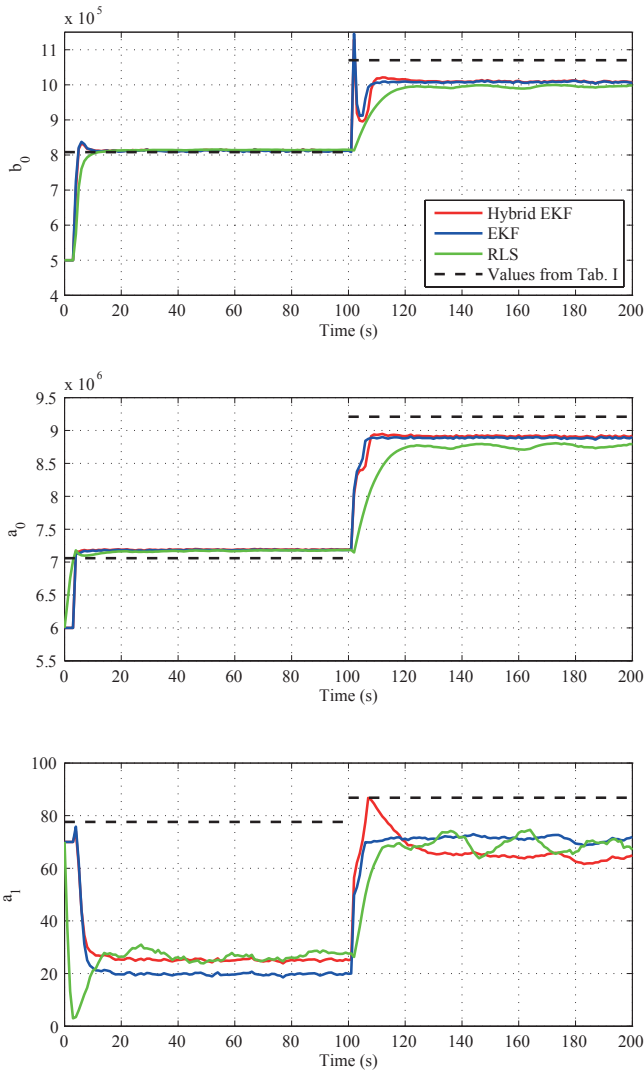


Fig. 7. Parameter estimates when using triangle wave excitation. The time-series have been downsampled to 1 Hz.

VII. DISCUSSION

The RLS method, the continuous EKF, and the hybrid EKF all perform well for parameter identification on this system. Judging by the results in Tab. II, the continuous EKF provides the best estimates overall. It is interesting to note that the parameters obtained using frequency response data provided the worst performance, suggesting that the parameters have changed in the brief period between each dataset were recorded, and that the optimal parameter values are dependent on the input signal.

For all the schemes the first transient is somewhat faster than the second transient. This is likely due to the step-like input experienced when the input signal was turned on, thus generating a large excitation which might have been beneficial with regards to convergence. When removing the mass, a brief, but fairly large, external disturbance was introduced in the measurements, introducing biases in the

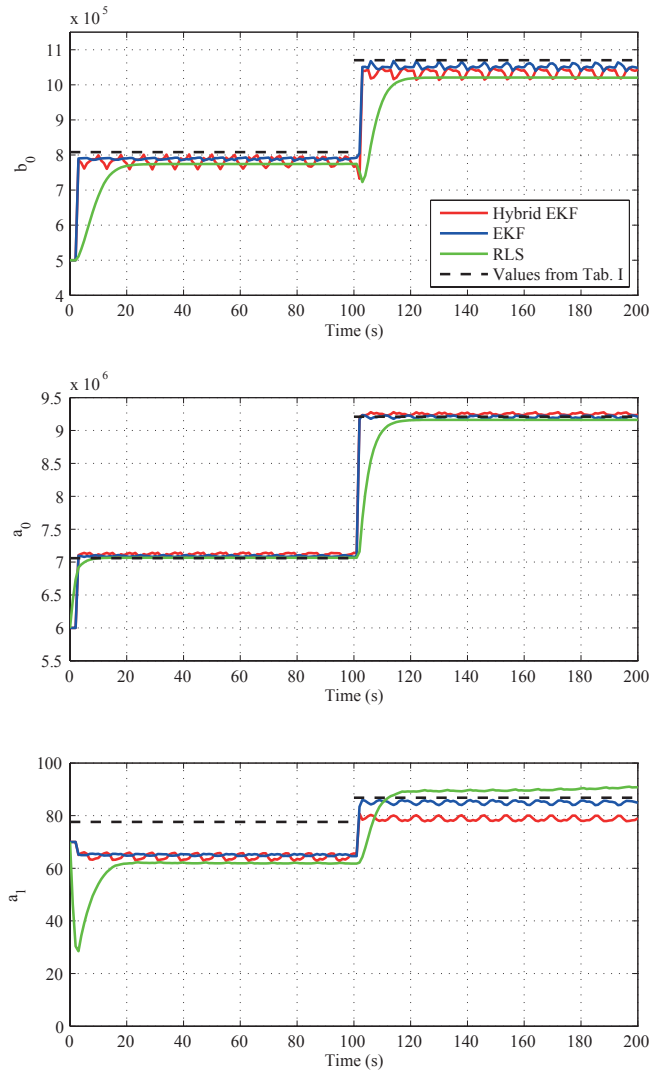


Fig. 8. Parameter estimates when using PRBS excitation. The time-series have been downsampled to 1 Hz.

parameter estimates.

Using PRBS excitation, all schemes converged to reasonable values, even without the pre-filter W_p and careful tuning of process noise covariance matrices used by the EKFs. Using the pre-filter and better tuning improved the results.

Using triangle wave excitation, none of the schemes converged to reasonable values without using a high-pass filter. Using a high-pass filter all schemes improved significantly. Using the resonant low-pass filter in addition to the high-pass filter, improved the results, especially the estimates obtained using RLS.

For the EKFs we observed that different covariance settings would lead to different, but small, biases in the parameter estimates. For some covariance settings the parameter estimates would diverge, this is in accordance with the results in [16].

When using PRBS excitation, the variance in the param-

eter estimates from the EKF was rather large. Reducing the covariances improved this, but too small covariances led to divergence, and the amount of reduction in parameter estimate variance was therefore limited. The RLS method had a much more consistent behavior in this regard.

The EKF provides a convenient method to trade off between speed of convergence and the variance in the parameter estimates, by tuning the process covariance matrix. Tuning the forgetting factor in the RLS method does not provide as dramatic effects on convergence speed, and it consistently seemed rather slow with regards to convergence speed. Using a non-normalized regressor speed up parameter convergence for RLS, but at the expense of larger transients and weaker properties for the signals in the estimation scheme.

As can be seen from Figs. 7 and 8, there are quite noticeable biases in the parameter estimates for each parameter identification scheme, and they also appear to depend on the excitation signal. Some bias should be attributed to the configuration of the pre-filter, W_p , as well as the tuning of the process noise covariance matrices. There is likely some influence from the hysteresis effect in the piezoelectric actuator, though most of this effect should be removed by the high-pass filter.

The parameter estimates found using the EKF are very similar, but most noticeably they differ in the obtained value for a_0 . This difference seemed rather consistent and not dependent on covariance tuning. The slightly different transient behavior, on the other hand, was tuning dependent. We conjecture that with more careful tuning, the transient behavior could have been made more similar.

The estimates produced by the RLS method are very much dependent on the pre-filter, and different filter configurations led to different biases. The RLS method produced noticeably different estimates than the EKF. Tuning the forgetting factor and the initial covariance matrix did only influence the transient behavior and the variance of the parameter estimates. The mean values obtained asymptotically were the same. The method requires numerical differentiation of the displacement signal, and the numerical differentiation method used might influence the results.

VIII. CONCLUSIONS

The RLS method, the continuous EKF, and the hybrid EKF all performed well for parameter identification on this system. The extended Kalman filters needed careful tuning to yield good performance, and all the schemes required some pre-filtration of the signals used to provide good results. The RLS method was particularly sensitive to the configuration of the pre-filter.

We found the continuous EKF to be the overall best performer, yielding parameter values that produced the least discrepancy between model response and measured response.

IX. ACKNOWLEDGMENTS

The authors wish to thank Dr. Kam K. Leang for providing the positioning stage, and Fig. 1, Dr. Andrew J. Fleming for providing the amplifier, and Øyvind N. Stamnes for his helpful comments and feedback.

REFERENCES

- [1] A. Preumont, *Vibration Control of Active Structures: An Introduction*, 2nd ed. Kluwer Academic Publishers, 2002.
- [2] J. Maess, A. J. Fleming, and F. Allgöwer, "Model-based vibration suppression in piezoelectric tube scanners through induced voltage feedback," in *Proceedings of the American Control Conference, Seattle, WA, 2008*, pp. 2022–2027.
- [3] A. A. Eilsen and A. J. Fleming, "Passive shunt damping of a piezoelectric stack nanopositioner," in *Proceedings of the American Control Conference, Baltimore, MD, 2010*, pp. 4963–4968.
- [4] S. Devasia, E. Eleftheriou, and S. O. R. Moheimani, "A survey of control issues in nanopositioning," *Control Systems Technology, IEEE Transactions on*, vol. 15, no. 5, pp. 802–823, 2007.
- [5] A. J. Fleming, S. Aphale, and S. O. R. Moheimani, "A new robust damping and tracking controller for spm positioning stages," in *Proceedings of the American Control Conference, St. Louis, MO, 2009*, pp. 289–294.
- [6] T. Ando, "Control techniques in high-speed atomic force microscopy," in *Proceedings of the American Control Conference, Seattle, WA, 2008*, pp. 3194–3200.
- [7] W. J. Karnavas, P. J. Sanchez, and A. T. Bahill, "Sensitivity analyses of continuous and discrete systems in the time and frequency domains," *Systems, Man, and Cybernetics, IEEE Transactions on*, vol. 23, no. 2, pp. 488–501, 1993.
- [8] L. Ljung, *System Identification: Theory for the User*, 2nd ed. Prentice Hall, Inc., 1999.
- [9] M. Gautier and P. Poignet, "Extended kalman filtering and weighted least squares dynamic identification of robot," *Control Engineering Practice*, vol. 9, no. 5, pp. 1361–1372, 2001.
- [10] P. A. Ioannou and J. Sun, *Robust Adaptive Control*. Prentice Hall, Inc., 1995.
- [11] D. Simon, *Optimal State Estimation*. Wiley-Interscience, 2006.
- [12] A. Gelb, Ed., *Applied Optimal Estimation*. The MIT Press, 1974.
- [13] R. G. Brown and P. Y. C. Hwang, *Introduction to Random Signals and Applied Kalman Filtering*. Wiley-Interscience, 1997.
- [14] H. W. Sorenson, "Least-squares estimation: from gauss to kalman," *IEEE Spectrum*, pp. 63–68, July 1970.
- [15] K. Reif, F. Sonnemann, and R. Unbehauen, "An ekf-based nonlinear observer with a prescribed degree of stability," *Automatica*, vol. 34, no. 9, pp. 1119–1123, 1998.
- [16] L. Ljung, "Asymptotic behavior of the extended kalman filter as a parameter estimator for linear systems," *Automatic Control, IEEE Transactions on*, vol. 24, no. 1, pp. 36–50, 1979.
- [17] M. Boutayeb, H. Rafaralahy, and M. Darouach, "Convergence analysis of the extended kalman filter used as an observer for nonlinear deterministic discrete-time systems," *Automatic Control, IEEE Transactions on*, vol. 42, no. 4, pp. 581–586, 1997.
- [18] A. Fleming and A. G. Wills, "Optimal periodic trajectories for band-limited systems," *Control Systems Technology, IEEE Transactions on*, vol. 17, no. 3, pp. 552–562, 2009.
- [19] O. Egeland and J. T. Gravdahl, *Modeling and Simulation for Automatic Control*. Marine Cybernetics, 2002.